npj | climate and atmospheric science

Article

Published in partnership with CECCR at King Abdulaziz University

https://doi.org/10.1038/s41612-024-00587-4

Near-term projection of Amazon rainfall dominated by phase transition of the Interdecadal Pacific Oscillation

Yi Liu [1,2], Wenju Cai[1,2,3,4], Yu Zhang [1,5], Xiaopei Lin [1,5] ✉ & Ziguang Li [1,5] ✉

The Amazon basin experienced a prolonged drought condition during the 2010s, leading to a large-scale forest degradation destructive to ecosystems and human society. Elusive are issues as to whether the decadal drought is driven by external forcing or internal variability, and whether the drought will continue or recover soon. Using large ensemble simulations from a state-of-the-art climate model, here we find a negative-to-positive phase transition of the Interdecadal Pacific Oscillation (IPO) explains ~45% (~40–49%) of the observed decadal drought of Amazon rainfall since 2010, much greater than the role of external forcing (~12%). Constraining future IPO phase transition reduces the uncertainty by ~38% from a range of -0.73 to $+0.31$ mm day^{-1} decade^{-1} to a range of -0.42 to $+0.23$ mm day^{-1} decade^{-1}, of the near-term Amazon rainfall projection before 2040 under a mid-intensity emission scenario. Thus, the IPO plays a crucial role in the post-2010 drying and the near-term rainfall projection.

The Amazon basin accounts for less than 0.05% of the global land area but hosts ~40% of the global tropical rainforests[1–3] and ~15% of the freshwater input to the world oceans[4,5], and is therefore one of the most important components of the Earth's climate system. A robust seasonality is seen in the Amazon climate, alternating between wet and dry periods[6]: The rainy season, influenced by the South American monsoon[7,8], runs from austral summer to autumn[9], which provides the major water source for the hydrological cycle, agricultural irrigation, and billions of animals and residents[10,11]. Extreme rainfall change in the Amazon basin reduces the stability and diversity of local ecosystems and causes substantial life and economic losses[12,13]. Assessing Amazon rainfall is therefore of great importance in projecting changes in regional climate and biological environment.

Rainfall over the Amazon rainforest decreased rapidly in the past decade. In 2005, 2010, and 2015, prolonged and widespread droughts occurred, causing large-scale bushfires, forest degradation, biomass decline, species death, and dramatic socioeconomic loss[14–19]. The frequent occurrences of severe droughts have raised interest in the causes. Several lines of evidence suggest that sea surface temperature (SST) variations, including El Niño-Southern Oscillation (ENSO) and north tropical Atlantic warming, are responsible for unusually decreased rainfall on the interannual timescale[20–22]. During an El Niño event, anomalous SST warming develops in the central-eastern tropical Pacific, weakening the west-minus-east SST gradient in the tropical Pacific and the Walker circulation, suppressing the descending branch in the central-eastern equatorial Pacific and ascending branch in the tropical South America and Atlantic. The suppressed ascending branch reduces Amazon rainfall through weakening the deep convection over the land and blocking moisture transport from the ocean. In addition, anomalous SST warming in the north tropical Atlantic causes a northward displacement of the Intertropical Convergence Zone (ITCZ), reducing the Amazon rainfall.

Beyond the interannual anomalies, the Amazon rainfall can be influenced by decadal-to-multidecadal internal variability. For example, a positive phase of the Interdecadal Pacific Oscillation (IPO) weakens the Walker circulation and leads to more frequent and intense El Niño events, leading to a prolonged drying of the Amazon basin[23]. A strong correlation ($r = -0.70$; $p < 0.01$) between the time series of the IPO and Amazon rainfall during the period of 1950–2019 indicates a substantial IPO modulation on the decadal variation of Amazon rainfall (Supplementary Fig. 1). The Atlantic Multidecadal Oscillation (AMO) also plays a role, with its positive phase driving a northward shift of Atlantic ITCZ, decreasing the Amazon rainfall[24–26]. However, there is no agreement yet on the mechanism of the

[1]Frontiers Science Center for Deep Ocean Multispheres and Earth System/Physical Oceanography Laboratory/Sanya Oceanographic Institution, Ocean University of China, Qingdao, China. [2]CSIRO Environment, Hobart, TAS, Australia. [3]State Key Laboratory of Marine Environmental Science & College of Ocean and Earth Sciences, Xiamen University, Xiamen, China. [4]State Key Laboratory of Loess and Quaternary Geology, Institute of Earth Environment, Chinese Academy of Sciences, Xi'an, China. [5]Laoshan Laboratory, Qingdao, China. ✉e-mail: linxiaop@ouc.edu.cn; ziguangli@ouc.edu.cn

prolonged reduction of rainfall in the past decade. Specifically, whether external forcing or internal variability dominates in driving the decadal drought, and their relative contribution remains debatable[23,27].

Changing the hydrology of Amazonia in a warmer climate is another issue of concern. Climate models agree in projecting a drier Amazon with increasing frequency of droughts, as driven by the Pacific and Atlantic SST change on the long-term scale[28–30]. However, internal variability affects the near-term projection, but whether the effect of internal variability will overwhelm the near-term change induced by anthropogenic forcing is unknown. A more reliable projection of Amazon rainfall can be obtained by predicting the evolution of internal decadal variability.

Previous studies assessed Amazon rainfall change mostly based on the multi-model but single-member projections[28–31]. Under this approach, it is difficult to separate the role of internal variability from external forcing. Recent advances in the large ensemble project from individual models facilitate an assessment of contributions by internal variability under climate change[32]. In particular, employing a single-model initial-condition large ensemble simulation proves valuable for discerning the relative role of internal variability in near-term projections[33–35]. Here, we use a set of 100-member simulations from the latest Community Earth System Model Large Ensemble Project (CESM2-LENS)[36], to investigate whether and to what extent the recent Amazon drought is attributed to internal variability, and to assess its constraint on projected change before 2040. We find that the Interdecadal Pacific Oscillation (IPO) has dominated the decreasing Amazon rainfall in the past decades, and will constrain the near-term change.

Results

Internal variability rather than external forcing drives recent Amazon drought

Whether the recent drought condition in the Amazon basin is driven by external forcing or internal variability is an important issue but remains elusive. The 100-member CESM2-LENS experiments are used to address this issue, which are under the same external forcing of historical anthropogenic and natural forcing (1850–2014) and future greenhouse gas forcing (2015–2100) but different oceanic and atmospheric initial states[36]. We take the ensemble mean of all members as the external forcing signal and the inter-member differences as the internal variability signal. We examine the change of Amazon wet-season (December-April, DJFMA) rainfall during 2010–2019 in observation and CESM2-LENS. Observed rainfall change features a significant decrease in much of the Amazon basin, with an averaged reduction of −0.80 mm day^{-1} decade^{-1} which is statistically significant above the 95% confidence level (Fig. 1a, b). The externally-forced rainfall change represented by the ensemble mean is however weak and insignificant over the Amazon basin, with a slight reduction of −0.098 mm day^{-1} decade^{-1}, which only explains ~12% of the observed drought (Fig. 1a, c). Rainfall change from internal variability, represented by the differences of individual members, exhibits a wide range from −0.97 to +0.63 mm day^{-1} decade^{-1} encompassing the observed drought rate (Fig. 1a).

We focus on two sub-ensembles with 10 members of the largest negative and positive rainfall changes, respectively (hereafter “dry10” and “wet10”). The dry10 members produce a significant decrease in rainfall over the Amazon basin, with a sub-ensemble mean reduction of −0.69 mm day^{-1} decade^{-1} comparable to the observation (Fig. 1a, d). The wet10 members show an opposite situation with significantly wetting over the basin and a sub-ensemble mean increase of +0.51 mm day^{-1} decade^{-1} (Fig. 1a, e). Such contrasting changes again highlight the role of internal variability in modulating the rainfall change in the Amazon basin. Therefore, the observed reduction of Amazon rainfall in the past decade, which is in part driven by external forcing, can be masked by internal variability.

Dominant influence of the IPO

To identify which internal variability dominates the Amazon drought in the recent decade, we examine the SST change during the same period of 2010–2019 in both observation and CESM2-LENS. The CESM2-LENS simulate a realistic mean state of Amazon rainfall compared with observation (Supplementary Fig. 2), and a reasonable connection between the IPO and Amazon rainfall, with an ensemble mean correlation coefficient of −0.48 during the period of 1950–2019 (Supplementary Fig. 3). The observed SST change is characterized by a positive-IPO-like pattern in the Pacific (Fig. 2a), while the ensemble mean SST change shows no well-defined spatial pattern but nearly homogeneous warming (Fig. 2b). By contrast, the dry10 members exhibit an SST warming in the central-eastern tropical Pacific, reminiscent of a positive IPO in the tropical region (Fig. 2c). We calculate the SST change difference of sub-ensemble mean between the dry10 and wet10 members, which resembles the positive-IPO-like pattern with a strong pattern correlation ($r = 0.72$; $p < 0.01$ based on the Cross-Correlation Function test) with the observation (Fig. 2d). We also find a significant negative correlation ($r = -0.56$; $p < 0.01$ based on the Cross-Correlation Function test) between changes of the IPO and Amazon rainfall among 100 members (Supplementary Fig. 4a). Such a coherent relationship can be seen in the 2000-year pre-industrial control run of CESM2 (Supplementary Fig. 5). In contrast, other internal variability such as the AMO, does not show a significant correlation (Supplementary Fig. 4b). These lines of evidence support a dominant influence of the IPO on the decreasing Amazon rainfall in the recent decades.

We use CESM2-LENS to quantify the contribution of the IPO on the recent Amazon drought, by adjusting the phase transition of the IPO in each member according to the observed phase transition of the IPO trend during 2010–2019. First, we remove the member-simulated IPO-related Amazon rainfall change; then, we add the observed IPO-related Amazon rainfall change by compensating the difference from the observed IPO phase transition to the simulated IPO phase transition in each member. As such, the random evolution of IPO in each member is replaced by the observed IPO phase transition. We conduct a linear regression of Amazon rainfall variation onto the IPO over the period of 2010–2019. The adjusted Amazon rainfall change can be considered due to both external forcing and the observed IPO phase transition during 2010–2019. The ensemble mean of the adjusted Amazon rainfall reduction is −0.45 (−0.50 to −0.40) mm day^{-1} decade^{-1}, accounting for ~56% (~50–62%) of the observed change (red bar of “IPO” in Fig. 2e); the ensemble mean of IPO-induced Amazon rainfall reduction is −0.36 (−0.39 to −0.32) mm day^{-1} decade^{-1}, accounting for ~45% (~40–49%) of the observed change, which is much greater than contribution from external forcing and the AMO (blue bar of “IPO” in Fig. 2e). Moreover, the Amazon rainfall reduction is significantly enhanced and distinguishable from zero after the IPO adjustment (Fig. 2f), highlighting the crucial role of the observed IPO phase transition in driving the recent drought.

IPO-induced uncertainty in projected Amazon rainfall

Since the IPO greatly modulates observed Amazon rainfall change, we assess the extent to which the phase transition of the IPO might influence the projection of Amazon rainfall. The ensemble mean of CESM2-LENS displays a sustained decrease of Amazon rainfall under greenhouse warming in the 21st century, which is consistent with previous studies[22,28,29]; however, large uncertainty from internal variability exists across different members, especially for the near-term evolution of Amazon rainfall (Fig. 3a). We similarly take the sub-ensembles of ten members with driest and wettest rainfall trends over the period of 2020–2039. Despite a slight negative trend of −0.13 mm day^{-1} decade^{-1} in the ensemble mean, the dry10 and wet10 show an opposite trend of −0.47 and +0.16 mm day^{-1} decade^{-1}, respectively (Fig. 3a). The difference of rainfall trends between dry10 and wet10 is significant and much greater than externally-forced trend (Fig. 3b, c). Hence, it is important to reduce the uncertainty in the near-term projection of Amazon rainfall.

To illustrate some uncertainty of near-term projection comes from the IPO, we show the spatial pattern of SST trend during 2020–2039. The ensemble mean SST trend depicts a well-defined El Niño-like warming pattern in the equatorial Pacific but homogeneous warming in other basins (Fig. 3d). The difference of SST trends between dry10 and wet10, however, resembles a positive-IPO-like pattern with warming in the central-eastern

equatorial Pacific but cooling in the northwestern and southwestern Pacific (Fig. 3e). We regress the projected grid-point rainfall and SST trends against projected Amazon rainfall trend during 2020–2039 for the inter-members. There is a prominent negative rainfall anomaly center over the Amazon basin, in association with the positive IPO-like pattern in the Pacific (Supplementary Fig. 6). Thus, the influence of the IPO is the largest uncertainty source of near-term projection of Amazon rainfall.

Near-term projection of Amazon rainfall constrained by the IPO

Because a phase transition of the IPO leads to large uncertainty in the near-term projection of Amazon rainfall, we can narrow the projection uncertainty by removing the IPO's influence. To quantify how much the uncertainty of the projected Amazon rainfall trend is contributed by the IPO phase transition, we removed the IPO's influence by taking out the linear regression of Amazon rainfall variation onto the IPO from the original Amazon rainfall trend during 2020–2039 in each member, so that the rest of rainfall trend is contributed by external forcing and other internal variability. The probability distribution of Amazon rainfall trends narrows after excluding the IPO's influence, with the spread reduced by ~38% from a range of −0.73 to +0.31 mm day^{-1} decade^{-1} to a range of −0.42 to +0.23 mm day^{-1} decade^{-1}, translating to a reduction of 31% in the inter-member SD from 0.182 to 0.126, or a reduction of 22% in the spread between the 5th and 95th percentile values from 0.58 to 0.45 mm day^{-1} decade^{-1} (Fig. 4a).

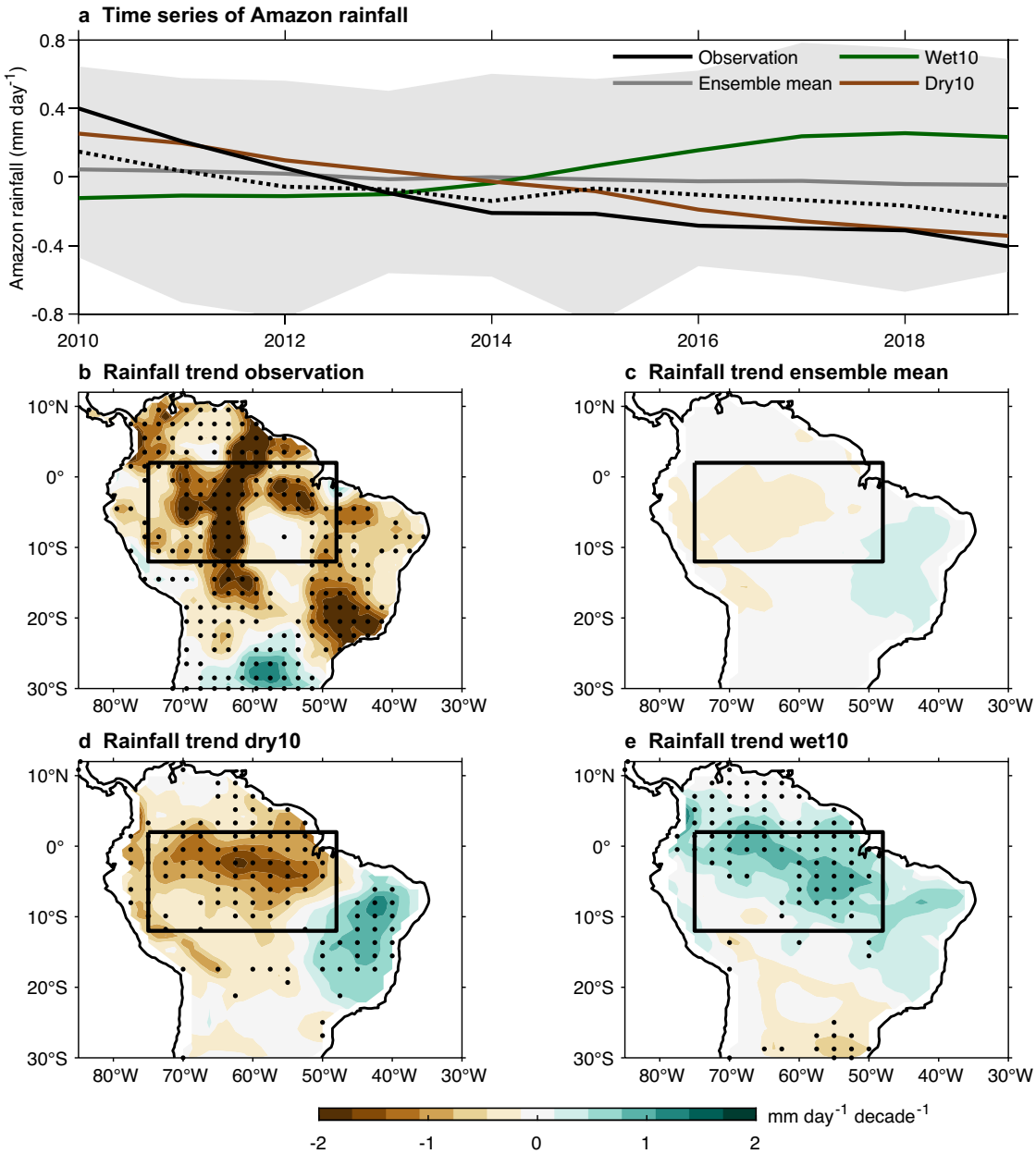

Fig. 1 | Observed and model-simulated trends of Amazon rainfall during 2010–2019. a Time series of 9-year running mean DJFMA Amazon rainfall anomalies (averaged over 12°S-2°N, 75°W-48°W) from observation (black line), ensemble mean of CESM2-LENS (gray line), sub-ensemble mean of 10 members with the wettest trends ("wet10", green line) and driest trends ("dry10", brown line) during the period of 2010–2019. Shading shows the SD of inter-member spread, indicating the effect of internal variability. **b** Spatial pattern of observed DJFMA rainfall trends during the period of 2010–2019. Stipples denote the trend is statistically significant at the 95% confidence level by the Mann–Kendall nonparametric method. **c** Same as **b**, but for CESM2-LENS ensemble mean. Stipples denote the trend is statistically significant by whether at least 80 of 100 members agree with the sign of ensemble mean. **d**, **e** Same as **b**, but for d dry10 and e wet10 sub-ensemble mean. Stipples denote the trend is statistically significant at the 95% confidence level by the Student's *t*-test.

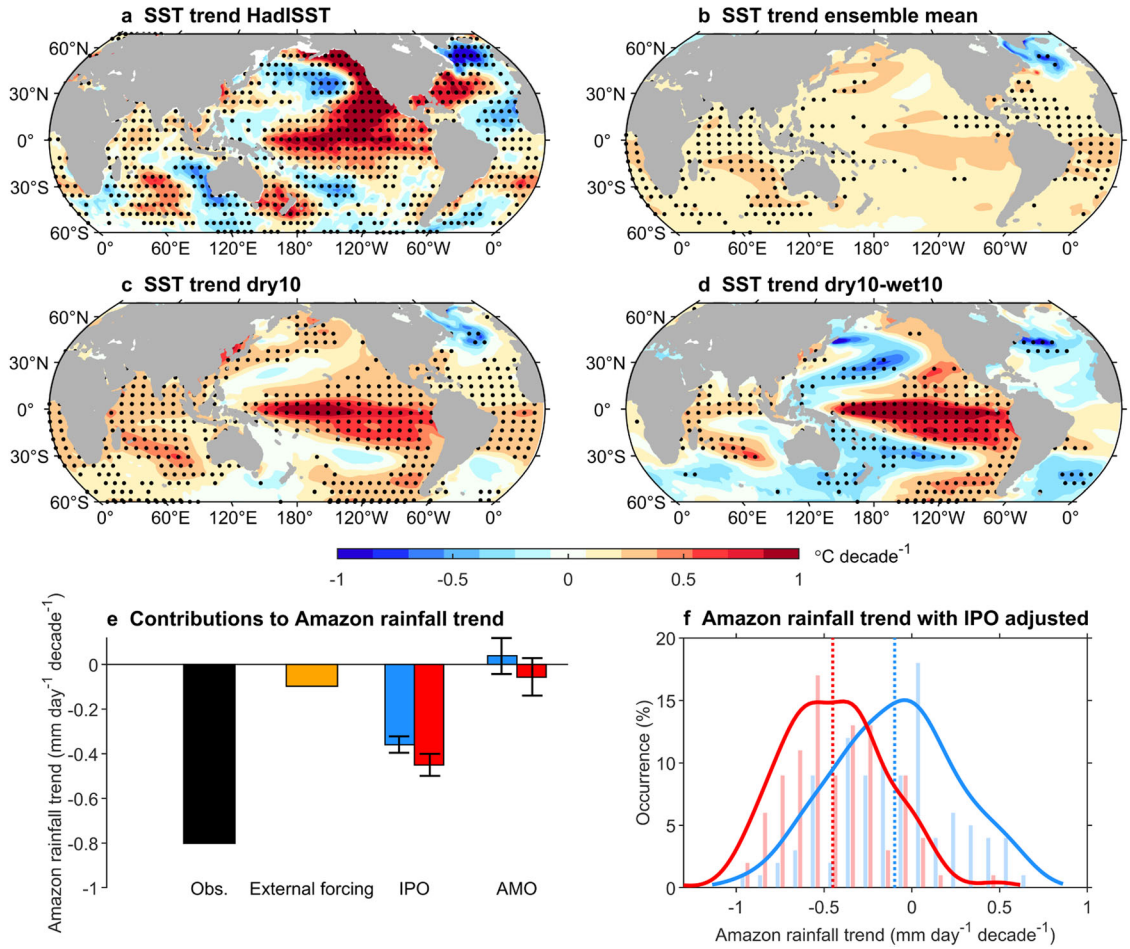

Fig. 2 | Contributions of the IPO to observed Amazon rainfall change during 2010–2019. a Spatial pattern of observed DJFMA SST trends during the period of 2010–2019. Stipples denote the trend is statistically significant at the 95% confidence level by the Mann–Kendall nonparametric method. **b** Same as a, but for CESM2-LENS ensemble mean. Stipples denote the trend is statistically significant by whether at least 80 of 100 members agree with the sign of ensemble mean. **c**, **d** Same as **a**, but for **c** dry10 and **d** difference between dry10 and wet10. Stipples denote the trend is statistically significant at the 95% confidence level by the Student's *t*-test. **e** From left to right are the observed (black bar), externally-forced (yellow bar), IPO-contributed, and AMO-contributed Amazon rainfall trends during the period of 2010–2019. The IPO/AMO-contributed trends are further divided into original IPO/AMO-related trends (blue bars) and total trends after IPO/AMO adjustment (red bars). Error bars show the 5th and 95th percentile of bootstrapped ensemble mean trends. **f** Histograms (bars) and fitted distribution (lines) of Amazon rainfall trend before (blue) and after the IPO adjustment. Dashed lines show the ensemble mean of the two distributions. The difference between the distribution before and after adjustment is statistically significant at the 95% confidence level by the Kolmogorov–Smirnov nonparametric test.

To depict the effect of the IPO on the projected Amazon rainfall trend, we assume a near-term phase transition of the IPO could be precisely predicted. Here we used a phase transition of the IPO from −0.5 °C to +0.5 °C (or vice versa) over 2020–2039. We add the impact of such a negative-to-positive (or positive-to-negative) IPO phase transition to the IPO-removed Amazon rainfall trend, by using the linear regression as mentioned above. Given a typical negative-to-positive IPO phase transition of +1 °C over the 20-year period, the 100 members show an ensemble mean of Amazon rainfall trend of −0.35 mm day^{-1} decade^{-1}, much greater than externally-forced ensemble mean of −0.13 mm day^{-1} decade^{-1} without such an IPO phase transition. A positive-to-negative IPO phase transition of −1 °C results in an ensemble mean of +0.12 mm day^{-1} decade^{-1}, which is in the opposite sign with the externally-forced trend. There is a 14% increase of probability (from 80 to 94%) with a decreasing Amazon rainfall trend in response to a +1 °C phase transition of the IPO, but a drop of 53% in probability (from 80 to 27%) for a −1 °C phase transition of the IPO (Fig. 4b).

Discussion

A 100-member large ensemble from CESM2 reveals that an IPO transition from negative-to-positive phase contributes to ~45% (~40–49%) of the observed decadal drought of Amazon rainfall since 2010, much greater than the role of external forcing (~12%). Further, the IPO evolution substantially affects the near-term projection of Amazon rainfall, introducing large uncertainty to the near-term projection. Such uncertainty reduces by ~38% after removing the IPO's influence. Thus, predicting the near-term phase transition of the IPO would greatly improve the projection of Amazon rainfall change in the coming decades. A reliable projection of Amazon rainfall change is essential for assessing regional climate change, evaluating the impacts, and managing the associated risks. In anticipation of the growing number of large ensemble simulations in the future, it becomes imperative to assess multi-model projection of near-term Amazon rainfall changes in order to reduce uncertainty from the single-model large ensemble approach.

Methods

Observational and model data

Monthly gridded rainfall observation is from Climatic Research Unit (CRU) v4.06, covering the period of 1950–2019 with a 0.5° horizontal resolution[37]. Monthly gridded SST data is from the Hadley Centre Sea Ice and Sea Surface Temperature dataset (HadISST) v1.1, covering the period of 1950–2019 with a 1° horizontal resolution[38]. Monthly anomalies of rainfall and SST referenced to the whole period are constructed by removing the monthly climatology.

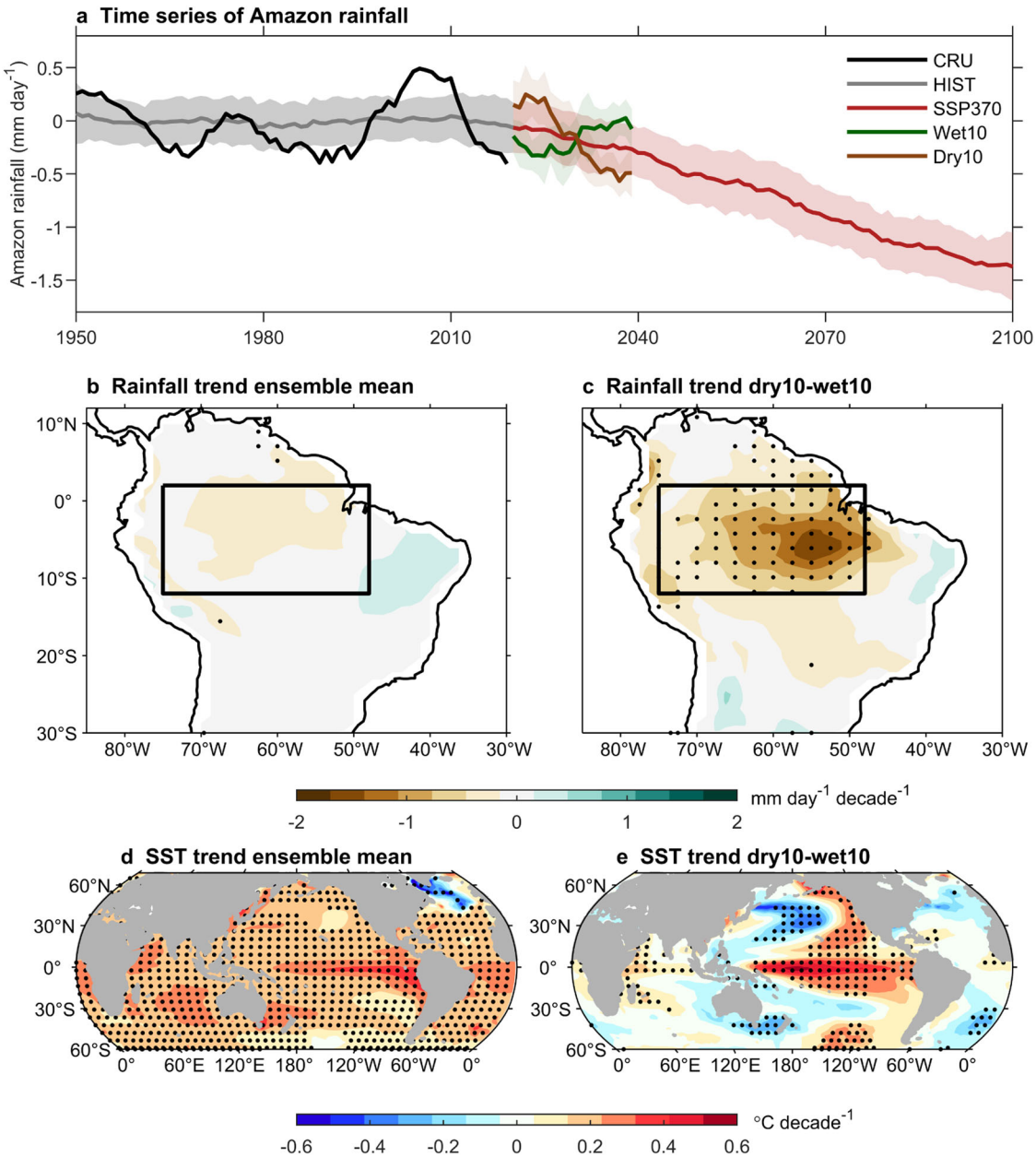

Fig. 3 | Projected Amazon rainfall change and associated SST trend in the near future. a Time series of 9-year running mean DJFMA Amazon rainfall anomalies from CRU (black line, 1950–2019) and CESM2-LENS ensemble mean under historical period (gray line, 1950–2019) and future SSP3–7.0 scenario (red line, 2020–2100). Green and brown lines denote the sub-ensemble mean of 10 members with the wettest trends (wet10) and driest trends (dry10) during the period of 2020–2039, respectively. Shading of each line shows the SD of inter-member spread indicating the effect of internal variability. **b**, **c** Spatial pattern of b ensemble mean of rainfall trend and c trend difference between dry10 and wet10 during 2020–2039. **d**, **e** Spatial pattern of **d** ensemble mean of SST trend and **e** trend difference between dry10 and wet10 during the period of 2020–2039. Stipples denote the trend that is statistically significant.

To assess the relative contributions of external forcing and internal variability, we use outputs from the large ensemble of Community Earth System Model 2 (CESM2-LENS), containing 100 members forced under historical anthropogenic and natural forcings up to 2014, and thereafter future greenhouse gas forcing under the Shared Socioeconomic Pathway (SSP) 3–7.0 emission scenario till 2100. Different mean states between 100 members are initialized to enable an assessment of oceanic and atmospheric contributions to ensemble spread[36]. The period of 2010–2019 focused in our study is connected by the period of 2010–2014 from historical simulations and 2015–2019 from SSP3–7.0 simulations. In addition, a 2000-year output from the pre-industrial control simulation of CESM2 is used to verify the decadal modulation of IPO on Amazon rainfall.

Separation of external forcing and internal variability

A 9-year running mean is applied to raw data in the observations and CESM2-LENS to extract decadal signals. Because all members run under the same external forcing, the ensemble mean of all members can be treated as the response to external forcing, and the inter-member difference can be regarded as arising from internal variability. For a climate variable X, the separation of external forcing and internal variability in member i can be described as:

$$X(i) = X_{\text{external}} + X_{\text{internal}}(i), i = 1, 2, \ldots, 100 \quad (1)$$

where X_{external} is the ensemble mean of 100 members, taken as the response to external forcing. $X_{\text{internal}(i)}$ is the residual of original $X(i)$ minus externally-

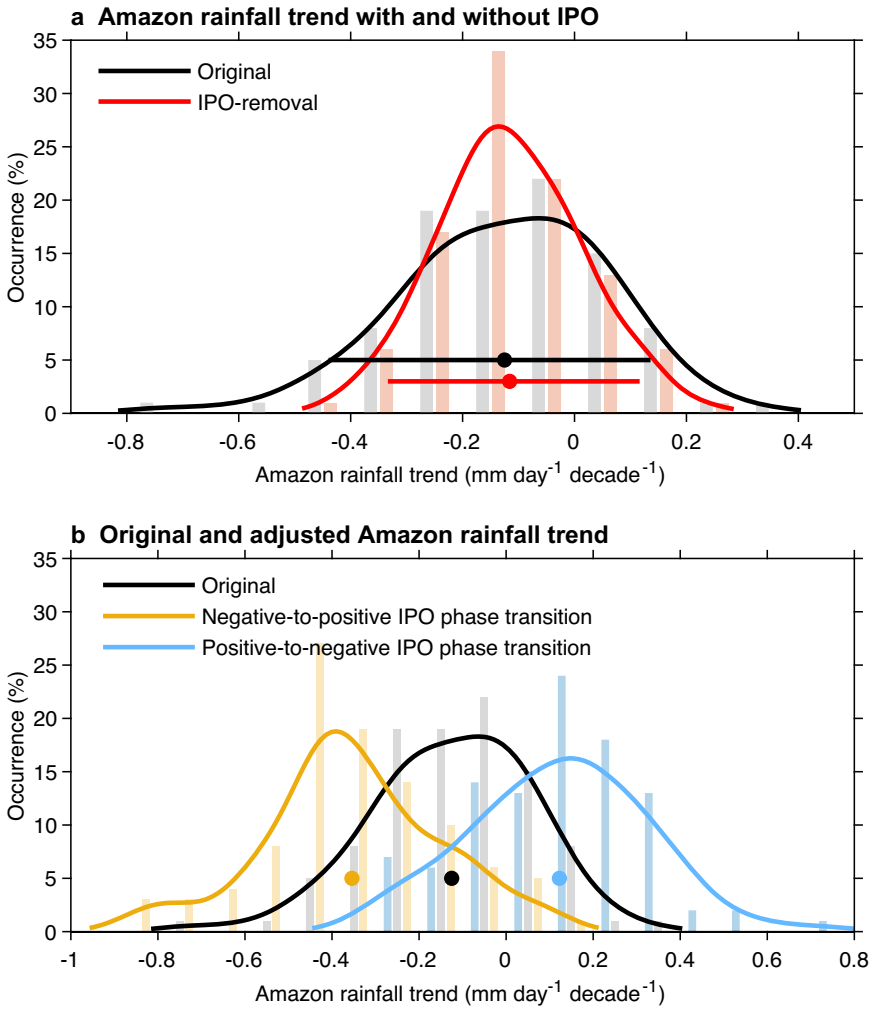

Fig. 4 | Projected Amazon rainfall trend adjusted by an IPO phase transition. a Histograms (bars) and fitted distribution (curves) of Amazon rainfall trend from 100 members during the period of 2020–2039. Gray bars and black curves denote the occurrences of the original Amazon rainfall trend; pink bars and red curves denote Amazon rainfall trends after removing the IPO's influence by linear regression. Black and red dots represent the ensemble mean of "original" and "IPO-removal" rainfall trend, respectively, together with horizontal lines showing the ranges of the 5th and 95th percentile in the two distributions. **b** Gray bars and black curve are the same as **a**, while the yellow and blue bars/curves denote Amazon rainfall trends adjusted by a common negative-to-positive IPO phase transition of +1 °C (yellow), and a common positive-to-negative IPO phase transition of −1 °C (blue), during 2020–2039. Black, yellow, and blue dots represent the ensemble mean of each distribution. These three distributions are significantly different from each other at the 95% confidence level by the Kolmogorov–Smirnov nonparametric test.

forced signal X_{external}, taken as the deviations in each member arising from internal variability.

Definition of climate indices

The Amazon rainfall index is calculated by the 9-year running mean of wet-season (December-April, DJFMA) rainfall anomaly averaged over the region of 12°S-2°N, 75°W-48°W (ref. 22). We define the IPO as the 9-year running mean of the Triple Pacific Index, which is the difference between the DJFMA SST anomaly averaged over the central-eastern equatorial Pacific (10°S-10°N, 170°E-90°W) and the average of the DJFMA SST anomaly in the northwestern (25°N-45°N, 140°E-145°W) and southwestern Pacific (50°S-15°S, 150°E-160°W)[39]. For observations, the IPO index is constructed using detrended SST anomaly; for each member i in CESM2-LENS, the IPO index is constructed using $SST_{\text{internal}}(i)$. We define the AMO as the 9-year running mean of DJFMA SST anomaly averaged over the North Atlantic Ocean (0°−65°N, 80°W-0°) with the global mean (80°S-80°N, 180°W-180°E) removal[40].

Quantifying IPO contribution to Amazon rainfall change

Here we utilize a well-documented approach based on the single-model initial-condition large ensemble simulation to quantify the contribution of IPO on Amazon rainfall change[33–35]. To evaluate the contribution of the IPO phase transition to the recently observed decadal drought of Amazon rainfall during 2010–2019, we adjust the IPO phase in different members to the observation during the same period. The adjusted Amazon rainfall change $\frac{\partial \text{AR}_{\text{adj}}(i)}{\partial t}$ is given by

$$\frac{\partial \text{AR}_{\text{adj}}(i)}{\partial t} = \frac{\partial \text{AR}_{\text{external}}}{\partial t} + \frac{\partial \text{AR}_{\text{internal-adj}}(i)}{\partial t}, i = 1, 2, ..., 100 \quad (2)$$

where $\frac{\partial \text{AR}_{\text{external}}}{\partial t}$ is the externally-forced Amazon rainfall change during 2010–2019. $\frac{\partial \text{AR}_{\text{internal-adj}}(i)}{\partial t}$ is the internally driven Amazon rainfall change after the adjustment of the IPO phase transition during 2010–2019, which is calculated by

$$\frac{\partial \text{AR}_{\text{internal-adj}}(i)}{\partial t} = \frac{\partial \text{AR}_{\text{internal}}(i)}{\partial t} + r_{\text{AR,IPO}}(i) \cdot \left(\frac{\partial \text{IPO}_{\text{obs}}}{\partial t} - \frac{\partial \text{IPO}(i)}{\partial t}\right)$$
$$r_{\text{AR,IPO}}(i) = \frac{\partial \text{AR}(i)}{\partial \text{IPO}(i)} \quad (3)$$

where $\frac{\partial \text{AR}_{\text{internal}}(i)}{\partial t}$ is the internally driven Amazon rainfall change before the adjustment of the IPO phase transition in member i during the period of 2010–2019, $r_{\text{AR,IPO}}(i)$ is the regression coefficient of Amazon rainfall index onto IPO index in member i during the period of 2010–2019. $\frac{\partial \text{IPO}_{\text{obs}}}{\partial t}$ is the observed change of IPO index during the period of 2010–2019, $\frac{\partial \text{IPO}(i)}{\partial t}$ is the simulated change of IPO index in member i during the period of 2010–2019. The relative contribution of IPO on observed decadal drought of Amazon rainfall is therefore taken as the percentage of the ensemble mean of $\frac{\partial \text{AR}_{\text{internal-adj}}(i)}{\partial t}$ to the observed change. Similar processes are applied to calculate the contribution of AMO.

To determine how much the IPO phase transition helps to constrain the uncertainty of Amazon rainfall trend in the near future, we extract and remove the Amazon rainfall trend induced by IPO phase transition by

$$\frac{\partial \mathrm{AR}_{\mathrm{non-IPO}}(i)}{\partial t} = \frac{\partial \mathrm{AR}(i)}{\partial t} - \frac{\partial \mathrm{AR}_{\mathrm{IPO}}(i)}{\partial t}$$
$$\frac{\partial \mathrm{AR}_{\mathrm{IPO}}(i)}{\partial t} = r_{\mathrm{AR,IPO}}(i) \cdot \frac{\partial \mathrm{IPO}(i)}{\partial t}, i = 1, 2, \ldots, 100 \quad (4)$$

where $\frac{\partial \mathrm{AR}_{\mathrm{non-IPO}}(i)}{\partial t}$ is the Amazon rainfall trend without IPO's influence in member i during the period of 2020–2039, $\frac{\partial \mathrm{AR}_{\mathrm{IPO}}(i)}{\partial t}$ is the IPO-contributed Amazon rainfall trend in member i during the period of 2020–2039, $\frac{\partial \mathrm{IPO}(i)}{\partial t}$ is the trend of IPO index in member i during the period of 2020–2039, and $r_{\mathrm{AR,IPO}}(i)$ is the regression coefficient of Amazon rainfall index onto IPO index in member i during the period of 2020–2039.

Data availability

Data related to the paper can be downloaded from the following: CRU v4.06 at https://crudata.uea.ac.uk/cru/data/hrg/; HadISST v1.1 at https://www.metoffice.gov.uk/hadobs/hadisst/; CESM2-LENS at https://www.earthsystemgrid.org/dataset/ucar.cgd.cesm2le.output.html;

Code availability

Codes for this study are available upon reasonable requests from the corresponding author.

Received: 3 November 2023; Accepted: 2 February 2024;
Published online: 26 February 2024

References

1. Laurance, W. F. et al. The future of the Brazilian Amazon. *Science* **291**, 438–439 (2001).
2. Aragão, L. E. et al. Environmental change and the carbon balance of Amazonian forests. *Biol. Rev.* **89**, 913–931 (2014).
3. Weng, W., Luedeke, M. K., Zemp, D. C., Lakes, T. & Kropp, J. P. Aerial and surface rivers: downwind impacts on water availability from land use changes in Amazonia. *Hydrol. Earth Syst. Sci.* **22**, 911–927 (2018).
4. Marengo, J. A. & Espinoza, J. C. Extreme seasonal droughts and floods in Amazonia: causes, trends and impacts. *Int. J. Climatol.* **36**, 1033–1050 (2016).
5. Nobre, C. A. et al. Land-use and climate change risks in the Amazon and the need of a novel sustainable development paradigm. *Proc. Natl Acad. Sci. USA* **113**, 10759–10768 (2016).
6. Zeng, N. Seasonal cycle and interannual variability in the Amazon hydrologic cycle. *J. Geophys. Res.* **104**, 9097–9106 (1999).
7. Liebmann, B. & Mechoso, C. R. The South American Monsoon System. In *The Global Monsoon System: Research and Forecast*, 2nd edn (eds. Chang, C. P. et al.) (World Scientific Publishing, 2010).
8. Marengo, J. et al. Recent developments on the South American monsoon system. *Int. J. Climatol.* **32**, 1–21 (2012).
9. Marengo, J. A., Liebmann, B., Kousky, V. E., Filizola, N. P. & Wainer, I. C. Onset and end of the rainy season in the Brazilian Amazon Basin. *J. Clim.* **14**, 833–852 (2001).
10. Marengo, J. A. On the hydrological cycle of the Amazon Basin: a historical review and current state-of-the-art. *Rev. Bras. Meteorol.* **21**, 1–19 (2006).
11. Leite-Filho, A. T., Soares-Filho, B. S., Davis, J. L., Abrahão, G. M. & Börner, J. Deforestation reduces rainfall and agricultural revenues in the Brazilian Amazon. *Nat. Commun.* **12**, 2591 (2021).
12. Betts, R. A., Malhi, Y. & Roberts, J. T. The future of the Amazon: new perspectives from climate, ecosystem and social sciences. *Philos. Trans. R. Soc. B.* **363**, 1729–1735 (2008).
13. Asner, G. P. et al. High-resolution forest carbon stocks and emissions in the Amazon. *Proc. Natl Acad. Sci. USA* **107**, 16738–16742 (2010).
14. Zeng, N. et al. Causes and impacts of the 2005 Amazon drought. *Environ. Res. Lett.* **3**, 014002 (2008).
15. Phillips, O. L. et al. Drought sensitivity of the Amazon rainforest. *Science* **323**, 1344–1347 (2009).
16. Lewis, S. L., Brando, P. M., Phillips, O. L., Van Der Heijden, G. M. & Nepstad, D. The 2010 amazon drought. *Science* **331**, 554–554 (2011).
17. Toomey, M., Roberts, D. A., Still, C., Goulden, M. L. & McFadden, J. P. Remotely sensed heat anomalies linked with Amazonian forest biomass declines. *Geophys. Res. Lett.* **38**, 19 (2011).
18. Jiménez-Muñoz, J. C. et al. Record-breaking warming and extreme drought in the Amazon rainforest during the course of El Niño 2015–2016. *Sci. Rep.* **6**, 33130 (2016).
19. Feldpausch, T. et al. Amazon forest response to repeated droughts. *Glob. Biogeochem. Cycles* **30**, 964–982 (2016).
20. Liebmann, B. & Marengo, J. Interannual variability of the rainy season and rainfall in the Brazilian Amazon Basin. *J. Clim.* **14**, 4308–4318 (2001).
21. Yoon, J.-H. & Zeng, N. An Atlantic influence on Amazon rainfall. *Clim. Dyn.* **34**, 249–264 (2010).
22. Cai, W. et al. Climate impacts of the El Niño–southern oscillation on South America. *Nat. Rev. Earth Environ.* **1**, 215–231 (2020).
23. Marengo, J. A. Interdecadal variability and trends of rainfall across the Amazon basin. *Theor. Appl. Climatol.* **78**, 79–96 (2004).
24. Villamayor, J., Ambrizzi, T. & Mohino, E. Influence of decadal sea surface temperature variability on northern Brazil rainfall in CMIP5 simulations. *Clim. Dyn.* **51**, 563–579 (2018).
25. Knight, J. R., Folland, C. K. & Scaife, A. A. Climate impacts of the Atlantic multidecadal oscillation. *Geophys. Res. Lett.* **33**, 17 (2006).
26. Wang, Y. & Huang, P. Potential fire risks in South America under anthropogenic forcing hidden by the Atlantic Multidecadal Oscillation. *Nat. Commun.* **13**, 2437 (2022).
27. Cox, P. M. et al. Increasing risk of Amazonian drought due to decreasing aerosol pollution. *Nature* **453**, 212–215 (2008).
28. Li, W., Fu, R. & Dickinson, R. E. Rainfall and its seasonality over the Amazon in the 21st century as assessed by the coupled models for the IPCC AR4. *J. Geophys. Res.* **111**, D2 (2006).
29. Duffy, P. B., Brando, P., Asner, G. P. & Field, C. B. Projections of future meteorological drought and wet periods in the Amazon. *Proc. Natl Acad. Sci. USA* **112**, 13172–13177 (2015).
30. Liu, Y., Cai, W., Lin, X. & Li, Z. Increased extreme swings of Atlantic intertropical convergence zone in a warming climate. *Nat. Clim. Chang.* **12**, 828–833 (2022).
31. Liu, Y., Li, Z., Lin, X. & Yang, J. C. Enhanced eastern Pacific ENSO-tropical north Atlantic connection under greenhouse warming. *Geophys. Res. Lett.* **48**, e2021GL095332 (2021).
32. Deser, C., Phillips, A., Bourdette, V. & Teng, H. Uncertainty in climate change projections: the role of internal variability. *Clim. Dyn.* **38**, 527–546 (2012).
33. Huang, X. et al. South Asian summer monsoon projections constrained by the interdecadal Pacific oscillation. *Sci. Adv.* **6**, eaay6546 (2020).
34. Huang, X. et al. The recent decline and recovery of Indian summer monsoon rainfall: relative roles of external forcing and internal variability. *J. Clim.* **33**, 5035–5060 (2020).
35. Wu, M. et al. A very likely weakening of Pacific Walker Circulation in constrained near-future projections. *Nat. Commun.* **12**, 6502 (2021).
36. Rodgers, K. B. et al. Ubiquity of human-induced changes in climate variability. *Earth Syst. Dynam.* **12**, 1393–1411 (2021).
37. Harris, I., Osborn, T. J., Jones, P. & Lister, D. Version 4 of the CRU TS monthly high-resolution gridded multivariate climate dataset. *Sci. Data* **7**, 109 (2020).
38. Rayner, N. et al. Global analyses of sea surface temperature, sea ice, and night marine air temperature since the late nineteenth century. *J. Geophys. Res.* **108**, D14 (2003).
39. Henley, B. J. et al. A tripole index for the interdecadal Pacific oscillation. *Clim. Dyn.* **45**, 3077–3090 (2015).

40. Trenberth, K. E. & Shea, D. J. Atlantic hurricanes and natural variability in 2005. *Geophys. Res. Lett.* **33**, 12 (2006).

Acknowledgements

The research was supported by the National Natural Science Foundation of China (42376022 and 41925025), and the Hainan Provincial Joint Project of Sanya Yazhou Bay Science and Technology City (2021JJLH0056). Y.L. was supported by the Fundamental Research Funds for the Central Universities (202261003) and the China Scholarship Council (202106330019). W.C. was supported by the Strategic Priority Research Program of the Chinese Academy of Sciences (XDB40030000). Y.Z. was supported by Laoshan Laboratory (LSKJ202202602), the Fundamental Research Funds for the Central Universities (202213050), and the project funded by China Postdoctoral Science Foundation (2021M703034).

Author contributions

Y.L., W.C., X.L., and Z.L. conceived this study. Y.L. performed all the analyses and wrote the initial manuscript with W.C. and Y.Z. All authors contributed to interpreting results, discussion and improvement of this paper.

Competing interests

The authors declare no competing interests.

Additional information

Supplementary information The online version contains supplementary material available at https://doi.org/10.1038/s41612-024-00587-4.

Correspondence and requests for materials should be addressed to Xiaopei Lin or Ziguang Li.